

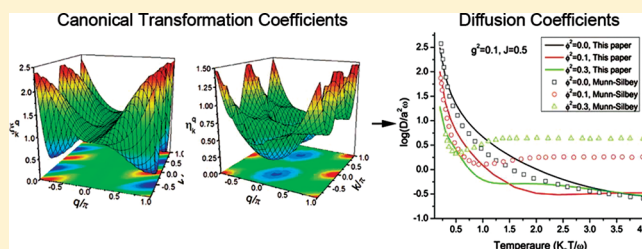
# On the Munn–Silbey Approach to Polaron Transport with Off-Diagonal Coupling and Temperature-Dependent Canonical Transformations

Dongmeng Chen,<sup>†,‡</sup> Jun Ye,<sup>†</sup> Haijun Zhang,<sup>†</sup> and Yang Zhao<sup>\*,†</sup>

<sup>†</sup>School of Materials Science and Engineering, Nanyang Technological University, Singapore 639798

<sup>‡</sup>College of Physics Science and Technology, China University of Petroleum, Dongying 257061, China

**ABSTRACT:** Improved results using a method similar to the Munn–Silbey approach have been obtained on the temperature dependence of transport properties of an extended Holstein model incorporating simultaneous diagonal and off-diagonal exciton–phonon coupling. The Hamiltonian is partially diagonalized by a canonical transformation, and optimal transformation coefficients are determined in a self-consistent manner. Calculated transport properties exhibit substantial corrections on those obtained previously by Munn and Silbey for a wide range of temperatures thanks to a numerically exact evaluation and an added momentum-dependence of the transformation matrix. Results on the diffusion coefficient in the moderate and weak coupling regime show distinct band-like and hopping-like transport features as a function of temperature.



## I. INTRODUCTION

Investigations on organic molecular crystals pioneered by Pope and co-workers<sup>1</sup> more than half a century ago made an immense impact on various fields of relevance in physics, chemistry, and materials science. The interplay between geometric and electronic structures has opened up novel materials with unlimited possibilities. The discovery of conducting properties of doped polyacetylene<sup>2</sup> in 1977 led to a Nobel prize in chemistry establishing a whole new field of organic electronics. After decades of research, many families of the organic semiconducting materials have been investigated. Among them, oligoacenes<sup>3–5</sup> and oligothiophenes<sup>6</sup> have been examined intensively due to the possibility of making single crystals with few defects via repeated sublimation processes. Single crystals of these materials can be used to develop transistors that allow for fundamental research on intrinsic properties as well as performance of organic electronic devices. The Holstein molecular crystal model was introduced in the 1950s<sup>7,8</sup> to account for the effect of electron–phonon interactions on transport. Since then, a lot of work has been carried out to deal with the complexities of the transport phenomenon in organic molecular crystals. As reviewed in ref 17, charge transport in organic semiconductors is governed by electronic coupling and electron–phonon interactions, and the main transport mechanism can be described by polaron and disorder models. Many theories on polaron transport are based upon a phenomenological model<sup>9</sup> or utilize the polaron effective mass approach.<sup>10</sup> However, the validity of these models is restricted to specific parameter ranges. More general microscopic models in understanding polaron transport were developed<sup>11–13</sup> from a density matrix approach, which is capable of describing electronic coupling and diagonal and off-diagonal electron–phonon interaction of arbitrary strength over a wide range of temperatures. The effect of off-diagonal coupling poses

many more difficulties to tackle than its diagonal counterpart, and as a result, off-diagonal coupling has not been extensively treated before.<sup>14</sup> More recently, microscopic models from generalized master equation approach,<sup>15</sup> and dynamical mean-field theory<sup>16</sup> have been developed.

Polaron transport theory developed by Holstein in his seminal work<sup>7,8</sup> was based upon perturbation expansions with its validity sometimes limited to cases of small transfer integrals.<sup>8</sup> Despite its limitation, the theory has been widely used for qualitative interpretations of experimental data, including the temperature dependence of the band-narrowing effect as well as the crossover from band-like behavior to hopping transport with increasing temperature. A microscopic transport theory that accounts for simultaneous diagonal and off-diagonal exciton–phonon coupling was developed by Munn and Silbey<sup>11–13</sup> on the basis of a canonical transformation of the Hamiltonian with an element of optimization. Off-diagonal coupling is found to increase the polaron binding energy and introduce new minima and broadening to the polaron band. In contrast, the effect of diagonal coupling is restricted to band narrowing. The Yarkony–Silbey variational approach<sup>20,21</sup> provides an attractive direction to solve the transport problems in organic molecular crystals. This approach has been borrowed to treat two phonon bands in a three-dimensional lattice by Parris and Kenkre.<sup>28</sup> However, as the Yarkony–Silbey approach lacks the flexibility in variational parameters; a more sophisticated approach is needed to capture the correct temperature dependence of diffusion coefficient and

**Special Issue:** Shaul Mukamel Festschrift

**Received:** September 29, 2010

**Revised:** December 28, 2010

**Published:** February 03, 2011

mobility. To obtain the optimal basis for a polaron system, the finite-temperature variational method by Cheng and Silbey<sup>18</sup> combining Merrifield's transformation with Bogoliubov's theorem has been recently devised, bringing substantial improvements to results obtained previously.<sup>13</sup> The theory is able to capture the universal band-like-to-hopping transition as temperature increases, and more importantly, a temperature-independent mobility at extremely low temperature has been found in agreement with a nonperturbative approach recently developed by Ortmann et al.<sup>22,23</sup> However, Merrifield's transformation itself is applicable only in the small polaron regime, and the off-diagonal exciton–phonon coupling was not accounted for in ref 18, making the approach insufficient to describe the phonon assisted transport/tunneling<sup>19</sup> in molecular crystals. Thus, further improvements are necessary for cases with simultaneous diagonal and off-diagonal coupling. Following up on the Munn–Silbey transformation method, Zhao et al.<sup>24–26</sup> devised a self-consistent routine to determine the transformation coefficients, demonstrating substantial corrections of the polaron band structure thanks to a built-in momentum dependence of the transformation coefficients. This serves as the starting point toward the evaluation of transport properties in this paper.

An attempt to extend the Holstein model to higher dimensions with a microscopic model has been made by Kenkre et al.,<sup>15</sup> utilizing the generalized master equation approach. This model was able to adequately explain the temperature dependence and anisotropy of measured mobilities in naphthalene. Using master equations, Wang et al.,<sup>27</sup> developed a nonperturbative method to handle the electron–phonon coupling fully quantum-mechanically and quantify charge-carrier transport properties in organic molecular crystals. A more sophisticated microscopic model based on a Hamiltonian of the Holstein–Peierls type has been presented by Bobbert and colleagues.<sup>29–31</sup> Very recently, a theory based on nonperturbative evaluation of Kubo formula for the carrier mobility<sup>22,32,33</sup> has been proposed, showing several improvements including the elimination of low-temperature singularity that often appears in theories based on narrow-band approximations. Based on a nonperturbative evaluation of the Kubo formula, calculations have been carried out for durene crystals<sup>34</sup> and guanine based materials,<sup>35</sup> and transport channels of charge carriers are revealed by making use of ab initio tools. Coupling to the intermolecular acoustic modes<sup>36</sup> was found to play a significant role in charge transport; thus the model presented by Bobbert et al. may be improved further. Experimental data of naphthalene can be well reproduced by this model with microscopic parameters obtained from ab initio calculations. However, this model neglects the intramolecular modes as well as the coupling of excitons to the intermolecular acoustic phonons, and only the coupling to the optical modes is accounted for. Moreover, the models developed by Bobbert et al., and by Munn and Silbey, are based on nonlocal canonical transformations with additional approximations. Thus the range of validity of these models still requires further exploration, despite some qualitative agreements with experiments. Hence, in the light of recent theories by Hultell et al.<sup>37</sup> and Troisi et al.,<sup>38</sup> it is clear that both local and nonlocal exciton–phonon interactions should be taken into account. A comprehensive theory of the charge transport in organic crystals requires treatments of the Hamiltonian having the lattice dealt with quantum mechanically to make itself valid for any temperature of interest, and the Munn–Silbey approach<sup>11–13</sup> combined with the self-consistent routine devised by Zhao et al.<sup>24</sup> provides a good opportunity to

explore the simultaneous effect of diagonal and off-diagonal exciton–phonon coupling on the transport properties of polaron.

The rest of the paper is organized as follows. The theoretical models are first introduced in section II, where the essential improvements over the original Munn–Silbey model have been proposed. In section III, the numerical results obtained with our approach have been discussed in detail and comparisons with previous results are made to illustrate the success of our approach. Finally, the conclusions are drawn in section IV.

## II. METHODOLOGY

The generalized Holstein Hamiltonian and its transformation have been described in detail previously by Munn and Silbey.<sup>11–13</sup> Here we will first discuss briefly the canonical transformation of the Hamiltonian, which yields a weak residual exciton–phonon coupling. Evaluation of correlation functions, essential to the final calculation of diffusion coefficient and mobility as a function of temperature, follows next. Our major focus in this paper will be the explicit form of the correlation functions, evaluation of critical exponential matrices and especially the transformation coefficients without resorting to the approximations in ref 12. In our study, the transformation coefficients are determined through solving a set of self-consistency equations, rather than an analytical form approximated in ref 12, therefore providing substantial corrections in the transport calculations. In section II A and B, expressions for the scattering and the hopping rates as well as the diffusion coefficients are introduced. Correlation functions are presented in section II C.

**A. Hamiltonian and its Transformation.** The generalized Holstein Hamiltonian incorporating simultaneous diagonal and off-diagonal coupling<sup>12</sup> has the form

$$H = \sum_n \varepsilon a_n^\dagger a_n + \sum_{n,m} J_{nm} a_n^\dagger a_m + \sum_q \omega_q (b_q^\dagger b_q + 1/2) + N^{-1/2} \sum_{nmq} \omega_q f_{nm}^q a_n^\dagger a_m (b_q + b_{-q}^\dagger) \quad (1)$$

Here  $a_n^\dagger(a_n)$  is the creation (annihilation) operator of an excitation (i.e., exciton or charge carrier) with energy  $\varepsilon$  at site  $n$ , and  $b_q^\dagger(b_q)$  creates (destroys) a phonon with frequency  $\omega_q$  and wave vector  $q$ .  $J_{nm}$  stands for the electronic transfer integral between sites  $n$  and  $m$ . In this study, the discrepancies between molecules have been neglected; thus the on-site energies are set to  $\varepsilon$ , as shown in eq 1. Finally, the exciton–phonon coupling is described by the last term of eq 1, where the coupling strength  $f_{nm}^q$  must satisfy the relationship  $(f_{n-m}^q)^* = e^{-iq \cdot (R_n - R_m)} f_{n-m}^q$  to make  $H$  Hermitian and translationally invariant.

A unitary transformation can be applied to the Hamiltonian, as shown below:

$$H \rightarrow \tilde{H} = U^\dagger H U \quad (2)$$

with

$$U = e^{N^{-1/2} \sum_{nmq} A_{nm}^q (b_{-q}^\dagger - b_q) a_n^\dagger a_m} \quad (3)$$

The transformation requires  $U^\dagger = -U$  to keep the translational symmetry of  $A_{nm}^q$ , similar to  $f_{nm}^q$ . Details of the transformation have been explicitly introduced in refs 11–13.

Moreover, the Hamiltonian in momentum representation is more convenient than the site representation due to the translational

symmetry. Equation 1 can be written in the momentum representation as

$$H = \sum_k \varepsilon_k a_k^\dagger a_k + \sum_q \omega_q (b_q^\dagger b_q + 1/2) + N^{-1/2} \sum_{kq} \omega_q f_{-k}^q a_{k+q}^\dagger a_k (b_q + b_{-q}^\dagger) \quad (4)$$

with  $\varepsilon_k = \varepsilon + J_k$  and

$$J_k = \sum_m e^{ik \cdot (\mathbf{R}_n - \mathbf{R}_m)} J_{nm} \quad (5)$$

where  $J_{nm} = J(\delta_{n,m+1} + \delta_{n,m-1})$ , and  $\omega_q$  is the phonon frequencies.

The exciton–phonon coupling coefficients can also be written as

$$f_k^q = \sum_m e^{-ik \cdot (\mathbf{R}_n - \mathbf{R}_m)} f_{n-m}^q \quad (6)$$

with the following coupling geometry:

$$f_k^q = g - i\phi[\sin(k) - \sin(k - q)] \quad (7)$$

which indicates that the antisymmetric type of coupling is used throughout the paper.

Now the transformation takes the following form in the momentum representation:

$$U = e^{N^{-1/2} \sum_{kq} A_{-k}^q (b_{-q}^\dagger - b_q) a_{k+q}^\dagger a_k} \quad (8)$$

and

$$A_k^q = \sum_m e^{-i(k-q) \cdot \mathbf{R}_n} e^{ik \cdot \mathbf{R}_m} A_{nm}^q = (A_{k-q}^q)^* \quad (9)$$

The transformation can then also be written as

$$U = e^{\sum_{kk'} a_k^\dagger S_{kk'} a_{k'}} \quad (10)$$

with

$$S_{kk'} = N^{-1/2} A_{-k}^{k-k'} (b_{k'-k}^\dagger - b_{k-k'}) \quad (11)$$

where  $S_{kk'}$  is an operator creating a net phonon with momentum  $k' - k$ . This operator is essential toward the evaluation of a series of important matrices, where

$$a_k \rightarrow \sum_{k'} \theta_{kk'} a_{k'} \\ a_k^\dagger \rightarrow \sum_{k'} \theta_{kk'}^\dagger a_{k'}^\dagger \quad (12)$$

with

$$\theta_{kk'} = [\exp(-\mathbf{S})]_{kk'} \\ \theta_{kk'}^\dagger = [\exp(\mathbf{S})]_{kk'} \quad (13)$$

where  $\mathbf{S}$  stands for matrix  $S_{kk'}$ . The transformed Hamiltonian can be partitioned into  $H_0$  terms (zeroth-order part) and the perturbative  $V$  terms. The thermal average of the  $\theta_{kk'}$  operator has the property:

$$\langle \theta_{k+k+q}^\dagger \theta_{k',k'+q} \rangle = \langle \theta_{k,k+q}^\dagger \theta_{k',k'+q} \rangle \delta_{qq'} \quad (14)$$

which ensures the correct thermal equilibrium behavior of  $H_0$  by keeping it diagonal in excitation wave vector.  $H_0$  here has

following expression:

$$\tilde{H}_0 = \sum_q \omega_q (b_q^\dagger b_q + 1/2) + \sum_k a_k^\dagger a_k \{ (\varepsilon - \tilde{J}_k) + N^{-1} \sum_q \omega_q |A_{-k}^q|^2 - 2N^{-1} \times \sum_{qk'} \omega_q f_{-k'}^q A_{-k}^q \langle \theta_{k'+q,k}^\dagger \theta_{k',k-q} \rangle + N^{-1/2} \times \sum_{qk'} \omega_q f_{-k'}^q A_{-k}^q \langle \theta_{k'+q,k}^\dagger \theta_{k',k} (b_q + b_{-q}^\dagger) \rangle \} \quad (15)$$

Here  $\tilde{J}_k$  represents the renormalized transfer integral which can be expressed by

$$\tilde{J}_k = \sum_{k'} J_{k'} \langle \theta_{k'k}^\dagger \theta_{k'k} \rangle \quad (16)$$

The perturbation parts of the transformed Hamiltonian can be written as

$$V = \sum_{kk'k''} \{ J_k T_{kk';kk''} - 2N^{-1} \sum_q \omega_q f_{-k}^q (A_{-k'}^q \times T_{k+q,k';k,k'-q} + N^{-1/2} \sum_q \omega_q f_{-k}^q a_{k+q}^\dagger a_{k'} \times [T_{k+q,k';kk''} (b_q + b_{-q}^\dagger) - \langle T_{k'+q,k';kk''} (b_q + b_{-q}^\dagger) \rangle] \} + N^{-1/2} \sum_{qk} \omega_q [A_{-k}^q - \sum_{k'} f_{-k'}^q \langle \theta_{k'+q,k}^\dagger \theta_{k',k-q} \rangle] \times (b_q + b_{-q}^\dagger) a_{k+q}^\dagger a_k \quad (17)$$

where

$$T_{kk';uu'} = \theta_{kk'}^\dagger \theta_{uu'} - \langle \theta_{kk'}^\dagger \theta_{uu'} \rangle \quad (18)$$

However, the last term of  $V$  has the potential to grow with increasing temperature, motivating the choice of  $A_k^q$ :

$$A_{-k}^q = \sum_{k'} f_{-k'}^q \langle \theta_{k'+q,k}^\dagger \theta_{k',k-q} \rangle \quad (19)$$

to curb this possible uncontrolled growth of  $\theta_{kk'}$ .

By applying the thermal average routine shown in ref 12, we can write the transformed Hamiltonian in a simpler form, which facilitates the numerical calculations. The zeroth-order Hamiltonian  $H_0$  now can be written as

$$\tilde{H}_0 = \sum_k \tilde{\varepsilon}_k a_k a_k + \sum_q \omega_q (b_q^\dagger b_q + 1/2) \quad (20)$$

and

$$\tilde{\varepsilon}_k = \varepsilon + \tilde{J}_k - N^{-1} \sum_q |A_{-k}^q|^2 \omega_q \quad (21)$$

The renormalized transfer integral in eq 21 is given by

$$\tilde{J}_k = \sum_{k'} \langle \theta_{k'} \rangle^2 (\exp E^0)_{kk'} J_{k'} \quad (22)$$

where the triadic  $E_{kk'}^q$  is a quantity introduced to yield a simpler form of the transformed Hamiltonian, with the following relationship:

$$E_{kk'}^q = N^{-1} (2n_{k-k'} + 1) (A_{k-q}^{k-k'})^* A_k^{k-k'} \quad (23)$$

here  $n_q$  is the Bose–Einstein distribution, with  $2n_q + 1 = \coth(\frac{1}{2}\beta\hbar\omega)$ .

With the form of  $A_k^q$  shown in eq 19, the perturbation part  $V$  of  $\hat{H}$  can be written as

$$V = \sum_{kk'k''} \{J_k T_{kk';kk''} - 2N^{-1} \times \sum_q \omega_q f_{-k}^q A_{-k'}^{-q} T_{k+q,k';k,k''-q} + N^{-1/2} \times \sum_q \omega_q f_{-k}^q T_{k+q,k';kk''} (b_q + b_{-q}^\dagger) a_{k'}^\dagger a_{k''}\} \quad (24)$$

In this study, the transformation coefficients  $A_k^q$  (A-matrix) will be obtained variationally prior to the calculations of the transport properties. The detailed numerical variational procedures can be found in ref 24. In performing the variational calculations, the transformation coefficients must satisfy following self-consistency equations together with eq 23:

$$\langle \theta_k \rangle = \exp \left[ -\frac{1}{2} \sum_{kk'} E_{kk'}^0 \right] \quad (25)$$

$$A_k^q = \langle \theta_{k-q} \rangle \langle \theta_k \rangle \sum_{k'} f_{k'}^q [\exp(E^q)]_{kk'} \quad (26)$$

The self-consistency equations above follow the Munn–Silbey secular elimination scheme. In ref 12, this set of equations was solved upon further approximations on  $A_k^q$ , whereas in this paper, it is solved numerically with an accuracy unavailable previously.

In the Munn–Silbey approach,<sup>12</sup> the transformation coefficients  $A_k^q$  were at first approximated by the scaling parameters  $\xi$  and  $\eta$  as

$$A_k^q = g\xi - i\phi\eta[\sin(k) - \sin(k-q)] \quad (27)$$

Numerical evaluation of the eqs 23–26 is facilitated by rewriting the eq 27 with real matrices  $\xi_k^q$  and  $\eta_k^q$  in the following form:

$$A_k^q = g\xi_k^q - i\phi\eta_k^q[\sin(k) - \sin(k-q)] \quad (28)$$

In the equation above, the sine function leads to zero imaginary part along the line with  $q = 0, 2k \pm \pi$ . In the numerical calculation, the lines with  $q = 0$  and  $q = 2k \pm \pi$  are treated as removable singularities. Moreover, the values of  $\eta_k^q$  along these lines are chosen to be analytically connected with neighboring values.<sup>24</sup> The variational matrices  $\xi_k^q$  and  $\eta_k^q$  chosen can preserve the symmetry properties of  $A_k^q$  in a way such that  $\xi_k^q = \xi_{k-q}^{-q}$  and  $\eta_k^q = \eta_{k-q}^{-q}$ .

The self-consistency approach shown in this paper is largely limited by the secular elimination scheme that is independent of the rigid-lattice tunneling matrix elements “ $J$ ”. However, since “ $J$ ” determines the rigid-lattice band structure and related quantities such as effective mass and density of states, this approach only applies for the narrow (rigid) band regime where the traditional small polaron theory is still available. The wide (rigid) band systems are beyond the scope of the approach discussed in this work. Based on the simple introduction and discussion of the Hamiltonian and transformation schemes, the parameters used for our numerical calculations are limited to the regime that holds the traditional small polaron scenario.

**B. Diffusion Coefficient.** The diffusion coefficient is closely related to the mean square displacement of an excitation in a given period of time. For the transformation scheme shown in

this paper, the mean square displacement can be calculated from the excitation density matrix. Approximations have been made to reduce the complexity of the exact formulism of the mean diffusion coefficient by neglecting small terms of the perturbation  $V$  as shown in the section above. The diffusion coefficient can then be expressed as<sup>11,13</sup>

$$D = a^2 \langle \langle v_k^2 / \Gamma_{kk} + \gamma_{kk} \rangle \rangle \quad (29)$$

where  $a$  is the nearest neighbor distance,  $\mathbf{k}$  is the wave vector, and  $v_k = \nabla_k E_k$ . The double bracket denotes the thermal average of the polaron states  $E_k$ , where  $\Gamma_{kk}$  and  $\gamma_{kk}$  are the scattering and hopping rates expressed as

$$\Gamma_{k'k} = N^{-1} \sum_{k \neq k'} W_{k,k';k'} \quad (30)$$

$$\gamma_{kk} = \frac{1}{2} \nabla_k^2 \sum_k \text{Re} \left( \frac{1}{2} W_{k,k;k'+q,k'+q} - W_{k,k+q;k',k'+q} \right) \Big|_{q=0} \quad (31)$$

where  $W_{k,k+q;k',k'+q}$ , crucial to the calculation of diffusion coefficient, are given by

$$W_{k,k+q;k',k'+q} = \int_0^\infty dt \{ \langle V_{k'+q,k+k+q} V_{k,k'}(t) \rangle \exp[-i(E_{k'+q} - E_{k+k+q})t] + \langle V_{k'+q,k+k+q}(t) V_{kk'} \rangle \exp[-i(E_k - E_{k'}t)] \} \quad (32)$$

Here the single angular bracket denotes the average of the residual interaction  $V_{kk'}(t)$  over phonon states. Using the formulism above, the evaluation of  $D$  will be done numerically here without introducing further approximations as in refs 11 and 12. With the diffusion coefficient  $D$ , the mobility can be easily obtained with the Einstein relation  $\mu = e\beta D$ .

**C. Correlation Functions.** As inferred from the expression of the diffusion coefficient, the central problem is the evaluation of the correlation functions  $\langle V_{k'+q,k+k+q} V_{k,k'}(t) \rangle$  since both the scattering and the hopping rates are determined by the  $W$  quantities. It is indicated from the previous formulism that the residual interaction  $V_{k,k'}(t)$  is closely related to the transformation coefficients  $A_k^q$ . Hence, the problem of evaluating  $D$  ultimately hinges on the solution of the self-consistency equations, i.e., eqs 23, 25, and 26. In this paper, the transformation coefficients that determine the structure of polaron states and energy bands are solved numerically, which provide new information about the transport properties of polarons in molecular crystals.

Without the analytical approximation form of  $\eta$  carried out in ref 13, the important quantity  $\langle \theta_{k,k'}^\dagger \theta_{q,q'} \rangle$  can be derived as<sup>12</sup>

$$\begin{aligned} \langle \theta_{k,k'}^\dagger \theta_{q,q'} \rangle &= \langle \theta_{-k'} \rangle \exp(D^{k-q})_{k,k'} \langle \theta_{-q'} \rangle \delta_{k-k', q-q'} \\ &= \langle \theta_{-k'} \rangle \exp(E^{k-q})_{-q', -q} \langle \theta_{-q'} \rangle \delta_{k-k', q-q'} \end{aligned} \quad (33)$$

and

$$(E^q)_{k,k'}[t] = \frac{1}{N} P_{k-k'}(t) (A_{k-q}^{k-k'})^* A_k^{k-k'} \quad (34)$$

$$(D^q)_{k,k'}[t] = \frac{1}{N} P_{k-k'}(t) (A_{k-q}^{k-k'})^* A_{-k'+q}^{k-k'} \quad (35)$$

where the expression of  $\langle \theta_k \rangle$  is given by eq 25.



The factors  $P_Q(t)$  are the characteristics of correlation functions for linear exciton–phonon coupling,<sup>39</sup> which may take the form

$$P_Q(0) = (2n_Q + 1)/N$$

$$P_Q(t) = [(2n_Q + 1) \cos(\omega t) + i \sin(\omega t)]/N \quad (36)$$

where  $n_Q$  is also the Bose–Einstein distribution, with  $(2n_Q + 1) = \coth^{1/2}(\hbar\omega/2k_B T)$  and  $\omega$  is the mean phonon frequency.

For the correlation to decay to zero at long times,  $P_Q(t)$  should be multiplied by a decay factor  $A(t)$ , defined as the Fourier transform of the phonon density of states, which takes a Gaussian form<sup>11</sup> as given by

$$A(t) = \exp(-\Delta^2 t^2/4) \quad (37)$$

where  $\Delta$  is the phonon bandwidth taken much less than  $\omega$ . For the convenience of numerical calculations, the mean phonon frequency  $\omega$  is set to 1. For all calculations performed in this paper,  $\Delta$  is set to be 0.1, indicating a rather narrow phonon band.<sup>11</sup> A number of factors can result in a finite bandwidth in the phonon density of states, and as pointed out by other authors,<sup>11,18</sup> the inclusion of the phonon bandwidth ensures the long-time decay of correlation functions.

In the evaluation of  $\langle V_{k'+q,k+q} V_{k,k'}(t) \rangle$ , an important quantity is the four  $\theta_k$  correlation function which is given by

$$\begin{aligned} & \langle \theta_{k_1,k_2}^+ \theta_{k_3,k_4} \theta_{q_1,q_2}^+ (t) \theta_{q_3,q_4} (t) \rangle \\ &= \sum_{r_1, r_2, r_3} \langle \theta_{k_2+r_1, k_2}^+ \theta_{k_3, k_3-r_1} \rangle \langle \theta_{q_2+r_2, q_2}^+ \theta_{q_3, q_3-r_2} \rangle \\ & \times [\exp(-E^{k_1+q_4+r_3-q_2-q_3}(t))]_{k_3+r_3-q_1-k_4-r_1, -q_2-r_2} \\ & \times [\exp(E^{k_1+r_2-q_3}(t))]_{-q_4-r_3, r_2-q_3} \\ & \times [\exp(E^{k_3-q_1-r_1}(t))]_{-q_1, k_3+r_3-q_1-k_4-r_1} \\ & \times [\exp(-E^{k_4-q_4-r_3}(t))]_{-q_4, -q_4-r_3} \\ & \times \delta_{k_1+q_1+k_4+q_4, k_2+q_2+k_3+q_3} \end{aligned} \quad (38)$$

Now we can derive the expression for  $\langle V_{k'+q,k+q} V_{k,k'}(t) \rangle$ , which is the core item of  $W$ . Here we first express  $V_{k,k'}$  as follows:

$$\begin{aligned} V_{k,k'} &= \sum_{\kappa} \left\{ J_{\kappa} T_{\kappa k, \kappa k'} - \frac{1}{\sqrt{N}} \sum_q \omega_q f_{-\kappa}^q \right. \\ & \times \left[ \frac{1}{\sqrt{N}} (A_{-\kappa}^{-q} T_{\kappa+q, k; \kappa, k'-q} + A_{-\kappa}^{q*} T_{\kappa+q, k+q; \kappa, k'}) \right. \\ & \left. \left. - \frac{1}{2} (T_{\kappa+q, k; \kappa, k'} \psi_q + \psi_q T_{\kappa+q, k; \kappa, k'}) \right] \right\} \end{aligned}$$

with

$$T_{k, k'; q, q'} = \theta_{k, k'}^+ \theta_{q, q'} - \langle \theta_{k, k'}^+ \theta_{q, q'} \rangle \quad (39)$$

and  $J_k = J \cos(k)$  denotes the polaron band with its width determined by  $J$ . As described in the previous section, the

currently applied approach is only applicable for narrow band rigid lattice system. Consequently, the value of  $J$  should not be too large to guarantee the accuracy of the transport results obtained.

The correlation function is now given by

$$\begin{aligned} \langle V_{k_1, k_2} V_{q_1, q_2}(t) \rangle &= \left\langle \sum_{k_3} \left\{ J_{k_3} T_{k_3, k_1; k_3, k_2} - \frac{1}{\sqrt{N}} \sum_{Q_1} \omega_{Q_1} f_{-k_3}^{Q_1} \right. \right. \\ & \times \left[ \frac{1}{\sqrt{N}} (A_{-k_1}^{-Q_1} T_{k_3+Q_1, k_1; k_3, k_2-Q_1} + A_{-k_1}^{Q_1*} T_{k_3+Q_1, k_1+Q_1; k_3, k_2}) \right. \\ & \left. \left. - \frac{1}{2} (T_{k_3+Q_1, k_1; k_3, k_2} \psi_{Q_1} + \psi_{Q_1} T_{k_3+Q_1, k_1; k_3, k_2}) \right] \right\} \\ & \times \sum_{k_4} \left\{ J_{k_4} T_{k_4, q_1; k_4, q_2} - \frac{1}{\sqrt{N}} \sum_{Q_2} \omega_{Q_2} f_{-k_4}^{Q_2} \right. \\ & \times \left[ \frac{1}{\sqrt{N}} (A_{-q_1}^{-Q_2} T_{k_4+Q_2, q_1; k_4, q_2-Q_2} + A_{-q_1}^{Q_2*} T_{k_4+Q_2, q_1+Q_2; k_4, q_2}) \right. \\ & \left. \left. - \frac{1}{2} (T_{k_4+Q_2, q_1; k_4, q_2} \psi_{Q_2} + \psi_{Q_2} T_{k_4+Q_2, q_1; k_4, q_2}) \right] \right\} \end{aligned} \quad (40)$$

The explicit expression of the correlation function has been given in the Appendix.

As read from the expression of the correlation function in eq 40, matrix coefficients  $A_k^q$  play an essential role toward an accurate evaluation of the correlation function. In ref 13, these coefficients were obtained only approximately, while in this paper, they are obtained numerically with unprecedented accuracy. One will find that the accurate evaluation of the  $A_k^q$  has dramatic influence on the overall transport calculations in the following section, especially for the cases with off-diagonal excitation-phonon coupling.

### III. RESULTS AND DISCUSSION

**A. Evaluation of Transformation Coefficients.** The numerical evaluation of transformation coefficients  $A_k^q$  involves the solution of the self-consistency equations eqs 23, 25, and 26. Details of the evaluation procedures have been discussed in detail in ref.,<sup>24</sup> here we only revisit some important issues related to the transport properties, especially the role of off-diagonal coupling.

For moderate temperature with  $k_B T = \hbar\omega$ , the self-consistency method applied in this paper tends to fail in strong coupling regimes; this is attributed to the failure to minimize errors to desired precision or to convergence to multiple solutions that are sensitive to procedure initialization. It is also possible for the convergence to fail in strong coupling regimes for solely numerical reasons. This problem increases with increasing exciton–phonon coupling, which leads to large positive and negative eigenvalues for the exponential matrices, thus to the possible failure of obtaining reliable diffusion coefficient. Due to the problems of convergence and possible multiple solutions of the method applied, we restricted our studies in the weak and intermediate coupling regimes to ensure the robustness of the results obtained.

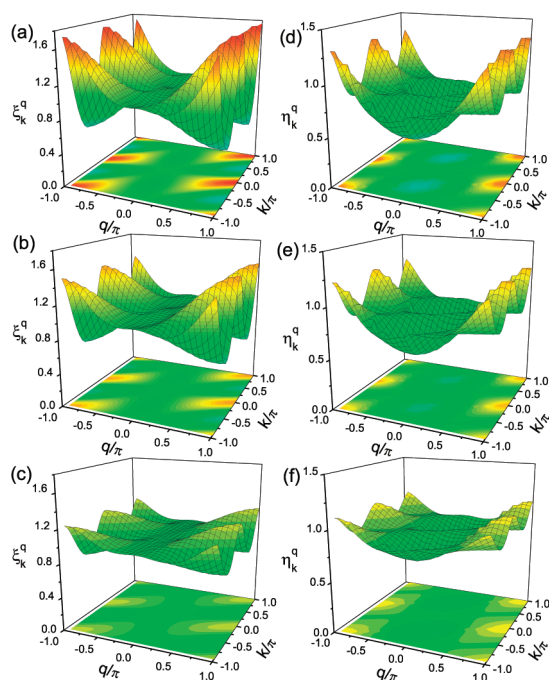


**Figure 1.** A-matrix parameters  $\xi_k^q$  (a)–(c) and  $\eta_k^q$  (d)–(f) as functions of increasing diagonal coupling strength  $g^2$ .  $g^2 = 0.1$  for (a) and (d), 0.3 for (b) and (e), and 1.0 for (c) and (f). Other parameters are  $J = 0.1$ ,  $\phi^2 = 0.3$ , and  $T = 1.0$ .

As demonstrated in ref 24, A-matrix parameters  $\xi_k^q$  and  $\eta_k^q$  in eq 28 obtained with the self-consistency procedure have a significant wave vector dependence, which is lacking in the original treatment of Munn and Silbey,<sup>12</sup> as indicated in eq 27. In addition, the Munn–Silbey parametrization of the A-matrix,  $\eta$  and  $\xi$ , can be regarded as the lower bounds of  $\xi_k^q$  and  $\eta_k^q$  rather than the average values. More importantly, the wave vector dependence of the variational parameters leads to significant changes in the structure of polaron energy band  $E_k$ , where the bimodal variation of  $E_k$  can be always found. Such changes in the structure of polaron states and the energy band lead to critical modifications of the transport properties, which will be explicitly examined in the next section. In this section, we present detailed structures of A-matrix parameters as well as the corresponding polaron bands obtained with the self-consistency routines, to facilitate understanding of calculated transport properties, which are deferred to the next subsection.

As shown in Figure 1, the two sets of A-matrix parameters in eq 28,  $\xi_k^q$  and  $\eta_k^q$ , differ in their wave vector dependence. In the vicinity of  $q = 0$ ,  $\xi_k^q$  is weakly structured and relatively flat with respect to  $k$ , while the wave vector dependence of  $\eta_k^q$  is much more pronounced than that of  $\xi_k^q$ . Regardless of coupling strength, the wave vector dependence of  $\xi_k^q$  and  $\eta_k^q$  has a characteristic “manta ray” shape, a fact that may be understood through an examination of the real-space structure of the A-matrix.<sup>24</sup>

As revealed in Figure 1, the A-matrix parameters tend to have less wave vector dependence for larger  $g$ . If diagonal coupling strength exceeds that of off-diagonal coupling, the parameters lose most of the  $q$  dependence. Thus, the transformation coefficients in eq 27, as approximated by Munn and Silbey,<sup>12</sup> represent the A-matrix in eq 28 in the limit of strong diagonal coupling. It is also interesting to look into the change of the polaron band structure (especially, band narrowing) as a function

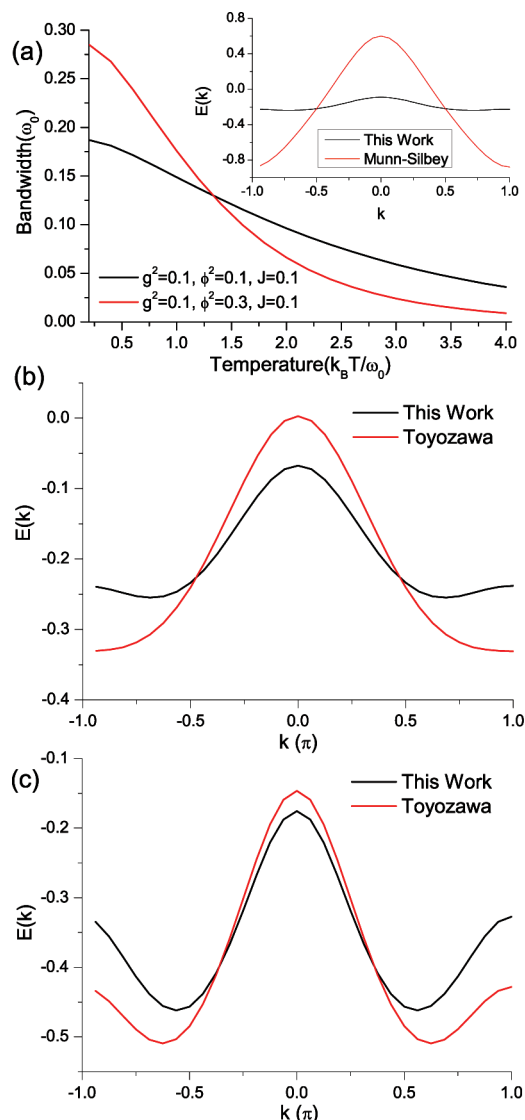


**Figure 2.** Polaron bandwidths (a) as functions of temperature, and band structures (b) and (c) comparisons between this work and the Toyozawa variational method with off-diagonal coupling strength (b)  $\phi^2 = 0.1$  and (c)  $\phi^2 = 0.3$  at  $T = 0$ , where  $g^2$  and  $J$  are both set to 0.1 for all calculations. The inset of (a) is the band structure comparison between the result from ref 12 by Munn and Silbey and that from this work at  $T = 1$  with  $g^2 = \phi^2 = J = 0.1$ .

of the temperature, which may provide an intuitive understanding of the difference between transport properties obtained here and those by Munn and Silbey using eq 27. Variance of the polaron bandwidth as well as the entire band with respect to temperature has been obtained with our numerically determined A-matrix and is illustrated in Figure 2. It is also indicated in the inset of Figure 2a that the polaron band obtained with the transformation coefficients of Munn and Silbey<sup>12</sup> lacks a bimodal structure and has a much larger bandwidth than that from the current approach. It is indeed counterintuitive to see that the greater momentum-space variability we find in our transformation coefficients should translate into a narrower polaron band. The explanation lies in that the binding energy is proportional to the average of  $|A_k^q|^2$ . Compared with results from ref 12, the average binding energy obtained in the current approach is

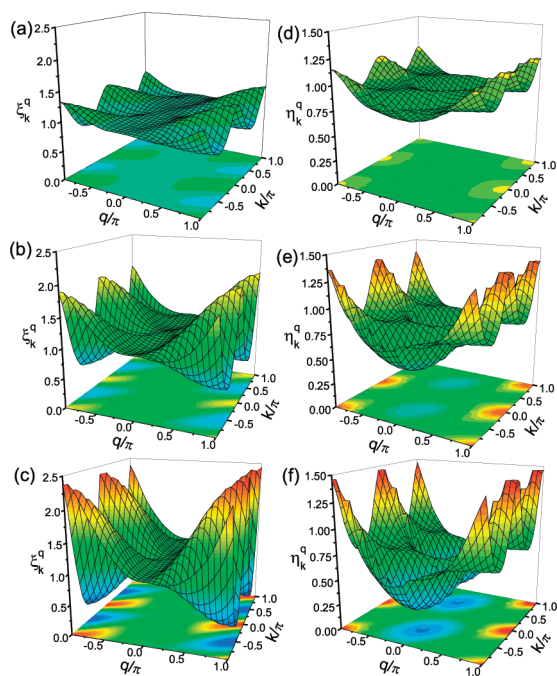


**Figure 3.** A-matrix parameters  $\xi_k^q$  (a)–(c) and  $\eta_k^q$  (d)–(f) as functions of increasing temperature.  $T = 0.2$  for (a) and (d), 1.3 for (b) and (e), and 4.0 for (c) and (f). Other parameters are  $J = 0.1$ ,  $g^2 = 0.1$ , and  $\phi^2 = 0.3$ .

significantly larger and the average Debye–Waller factor significantly smaller, which eventually leads to the narrower band.

To lend further support to the polaron band structure calculated here, it is helpful to introduce the Toyozawa Ansatz<sup>40,41</sup> for zero-temperature band comparisons. As shown in Figure 2b,c, good agreement between the current method and the Toyozawa Ansatz has been found. For weak diagonal and off-diagonal coupling, as is the case in Figure 2b, the Toyozawa method yields a larger bandwidth, and with increasing  $\phi$ , the bimodal structure appears and the agreement between the two approaches improves. The concurrence provides legitimacy to the current approach in finding reliable polaron bands, a step that is essential for the transport calculations. Moreover, the band narrowing effect is in good qualitative agreement with those obtained with the Holstein–Peierls model and ab initio calculations in ref 29. As can be readily seen from Figure 2a, the off-diagonal coupling strength helps boost the bandwidth for temperatures lower than  $\omega$ ,  $g^2 = 0.1$ , and  $J = 0.1$ .

To better understand the bandwidth narrowing effect, the parameter matrices  $\xi_k^q$  and  $\eta_k^q$  have been plotted in Figure 3 for three temperatures,  $T = 0.2$ , 1.3, and 4.0 in unit of  $\omega$ . Other control parameters in Figure 3 are set to be the same as those for Figure 2c. As temperature increases, the wave vector variations grow for both  $\xi_k^q$  and  $\eta_k^q$ , while in Figure 1, the variations are reduced as  $g$  increases. As explained in ref 24, a larger wave vector variation in  $\xi_k^q$  and  $\eta_k^q$  is transformed into a weaker distortion of the energy band, which explains the temperature dependence in Figure 2a. In contrast to an overall enhancement of polaron band-narrowing by including off-diagonal coupling in ref 29, our model demonstrates the possibility that at low temperatures off-diagonal coupling may increase the bandwidth while at high temperature the effect is reversed. Such an effect can be understood from eqs 21–26, where the bandwidth is shown to be closely related to the renormalized transfer integral  $\mathcal{J}_k$  and the

polaron binding energy, which is the third term on the right-hand side of eq 21. At lower temperatures, the binding energy dominates in eq 21 in the presence of off-diagonal coupling strength  $\phi$ , resulting in a bandwidth that increases with  $\phi$ . At high temperatures, however, the renormalized transfer integral  $\mathcal{J}_k$  dominates at weak off-diagonal coupling, and the bandwidth derived from the  $\mathcal{J}_k$  term shrinks with increasing  $\phi$ . While diagonal exciton–phonon coupling always acts as a localization factor, off-diagonal exciton–phonon coupling is a transport mechanism as it is an agent for polaronic localization. At low temperatures, the former trait of the off-diagonal coupling is more evident as the off-diagonal coupling alone can generate a polaron-bandwidth through the off-diagonal polaron binding energy term even in the absence of the transfer integral ( $J = 0$ ).

**B. Transport Properties.** The influence of the diagonal coupling strength  $g$  and off-diagonal coupling strength  $\phi$  (especially the latter) is substantial in determining momentum space modulations of transformation coefficients  $A_k^q$ , which in turn determine the structure of polaron states and the energy bands. For all calculations here, the number of sites is equal to 6 and the hopping integral  $J$  is 0.1 in units of  $\omega$  unless specified otherwise. Comparisons between the results obtained here and those from ref 13 have been made to illustrate the importance of the A-matrix momentum dependence as well as the straightforward numerical evaluation of transport properties sans additional approximations.

In the calculations of the transport properties, computation time increases dramatically with the number of sites. Our existing computational capabilities allow only calculations for less than 10 sites without overshooting memory requirements. To ensure the robustness of the results obtained with current method, we computed the diffusion coefficient  $D$  for 1D lattices of 4, 6, and 8 sites. The results with various lattice sizes and control parameters are displayed in Figure 4, indicating that almost identical results are obtained for lattices of 6 and 8 sites in the absence of off-diagonal coupling. Hence, in such a scenario, calculations with 6 sites are expected to give sufficiently reliable values of  $D$  at affordable computational cost. As  $\phi^2$  increases, however, the number of sites becomes an issue in determining the value of  $D$  due to exciton–phonon correlation spans over longer distances. The effect of the lattice size is more prominent in the low temperature regime as shown in Figure 4b,c, where the transport properties are dominated by coherent or band-like contributions. At higher temperatures, the hopping contribution eventually dominates the transport and the results become less sensitive to the system size. This can also be understood from polaron band narrowing at high temperatures and a reduced effective transfer integral with increasing temperature. As the diagonal coupling strength  $g$  increases, the difference between the results obtained with 4 sites and 6 sites becomes less obvious than the weak coupling cases. Even better agreement is reached for  $\phi^2 = 0$ , and the results are found to be almost identical from 4 to 8 sites, as shown in Figure 4d. It is also interesting to spot nonmonotonic changes of the diffusion coefficient (i.e., a “hump”) as a function of the temperature, in the absence of any size dependence, in the low temperature regime for  $g^2 = 0.5$  and nonzero  $\phi^2$ , as shown in Figure 4e,f. Such a hump also appears in Figure 4c for  $g^2 = 0.1$  and  $\phi^2 = 0.7$  despite a slightly visible size dependence of the diffusion coefficient. For a fixed value of  $g^2$ , the “hump” becomes more pronounced with increasing  $\phi^2$ , underlying the partial role of off-diagonal coupling.

As shown in Figure 5, increasing the phonon bandwidth  $\Delta$  leads to an increase in the band-like contribution to the diffusion coefficient, and a decrease in the relative importance of the



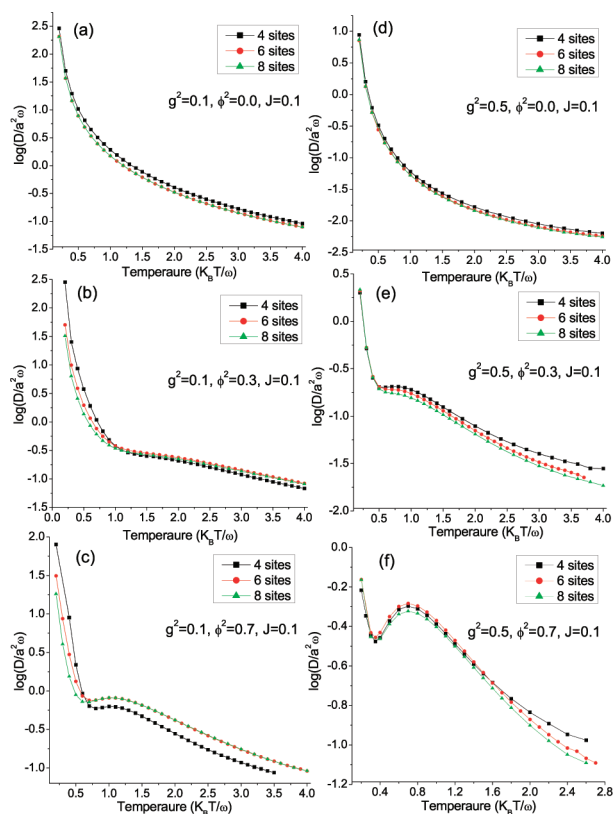


**Figure 4.** Diffusion coefficient  $D$  versus scaled temperature  $k_B T / \omega$  for a 1-dimensional chain with 4, 6, and 8 sites, where the diagonal coupling strength  $g^2 = 0.1$  for (a)–(c) and  $g^2 = 0.5$  for (d)–(f). The off-diagonal coupling strength  $\phi^2$  is equal to 0.0 for (a) and (d), 0.3 for (b) and (e), and 0.7 for (c) and (f). Finally, the transfer integral  $J = 0.1$  for all cases.

hopping contribution. These findings from our numerical calculations for a case of diagonal exciton–phonon coupling are in good agreement with analytical results from ref 11. Qualitatively similar results can be obtained with the inclusion of off-diagonal coupling.

In the original work of Munn and Silbey, the diffusion coefficient as a function of temperature have been studied with structureless  $\mathbf{A}$ -matrix parameters  $\xi$  and  $\eta$ . The detailed structure for the  $\mathbf{A}$ -matrix parameters is found to have a substantial impact on the transport properties, as revealed in Figure 6 by comparing the diffusion coefficients from ref 13 with those obtained here. Moreover, we would like to note that in the absence of off-diagonal coupling our results are in good agreement with those from refs 15 and 18. The results in this paper can be compared with those obtained using other methods such as a Green's function approach<sup>42</sup> and variational exact diagonalization with a better construction of phonon states.<sup>43</sup> For example, with an improved numerical technique in ref 43, the 1D polaron mass and radius are studied for an expanded parameter regime, where comparisons with our approach are especially convenient. Despite the discrepancies between our results and those of Munn and Silbey in the high temperature regime where hopping transport dominates, agreement is found in the low temperature regime where band-like transport prevails. This can be understood as follows. As discussed in ref 24, the transformation coefficients obtained self-consistently are shown to have stronger wave vector dependencies as  $\phi$  increases. For weak off-diagonal coupling, however, the average values of  $\xi_k^q$  and  $\eta_k^q$  generated by the self-consistency procedure are in reasonable agreement with those by Munn and Silbey<sup>12</sup> despite some systematic deviations, which leads

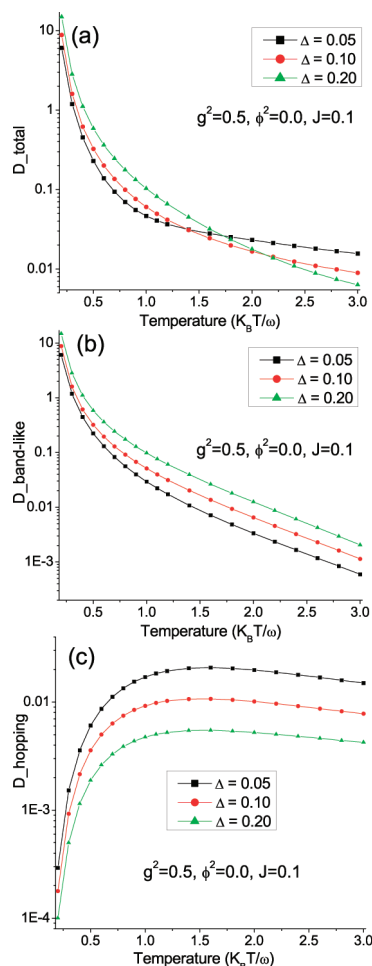


**Figure 5.** Effects of phonon bandwidth  $\Delta$  on (a) total diffusion coefficient, (b) band-like contribution, and (c) hopping contribution. Other parameters are  $g^2 = 0.5$ ,  $\phi^2 = 0.0$ , and  $J = 0.1$ .

to the aforementioned low-temperature agreement. As shown in Figures 2 and 3, a higher temperature induces a higher amplitude of wave vector variations of the  $\mathbf{A}$ -matrix parameters together with a much flatter polaron band as compared with its Munn–Silbey counterpart, resulting in a diminished diffusion coefficient. Finally, the diffusion coefficients obtained here in the absence of the off-diagonal coupling are shown to have qualitative agreements with those from ref 13. The differences between the two can be ascribed to a series of approximations made in ref 13 leading to the calculation of the diffusion coefficient, which in this work are substituted with numerically exact evaluations.

#### IV. CONCLUSIONS

Within the framework of the Munn–Silbey approach to polaronic transport in organic molecular crystals, diffusion coefficients have been computed by numerical means while taking into account simultaneous diagonal and off-diagonal exciton–phonon coupling for a wide range of temperatures. With the transformation coefficients determined self-consistently without the additional approximations found in refs 12 and 13 calculated transport properties exhibit substantial corrections on those obtained previously thanks to the added momentum dependence of the  $\mathbf{A}$ -matrix parameters and numerically exact evaluation of many essential quantities. The general transport properties obtained are also in



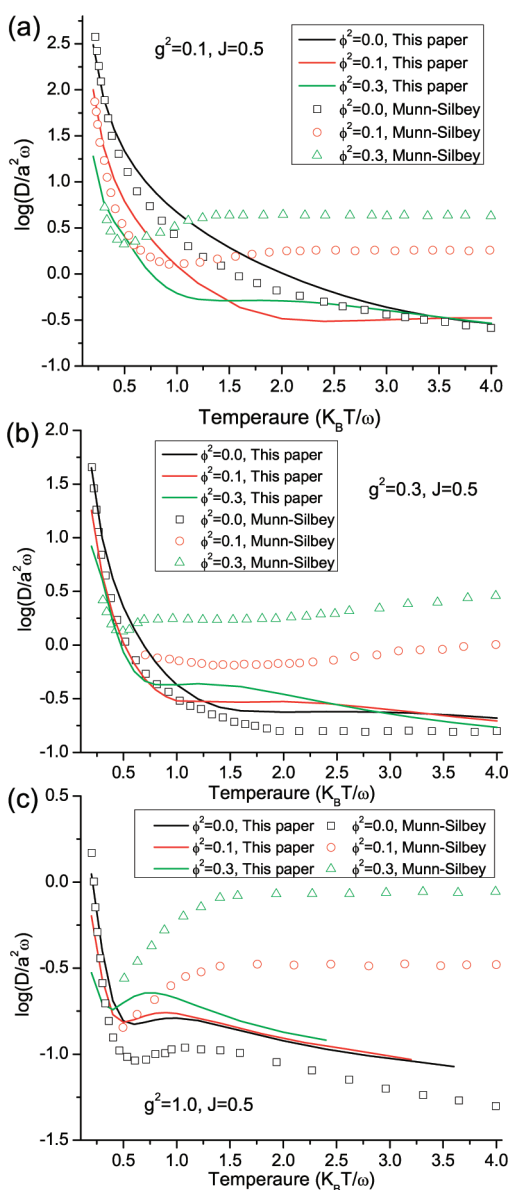


**Figure 6.** Comparisons of the logarithm diffusion coefficient of this work and those from ref 13, where both diagonal and off-diagonal couplings are limited to a moderate value to guarantee the definiteness of our results.

good qualitative agreement with those obtained with the Holstein–Peierls model and ab initio calculations,<sup>29</sup> demonstrating robustness of the current approach.

Comparisons between this work and the one in ref 13 reveal the importance of the electron–phonon correlations and the polaron band structure to transport properties of the extended Holstein molecular crystal model. By treating the diagonal and off-diagonal exciton–phonon coupling on an equal footing in our self-consistency procedure, the current approach is one of the few capable to model realistically the transport phenomenon in organic molecular crystals, for which the effect of off-diagonal coupling often cannot be neglected. Off-diagonal coupling, in itself, is a transport mechanism, as it is an agent for polaronic localization. Inclusion of off-diagonal coupling in the current approach allows us to see the critical role it plays in determining both polaron structures and transport properties over a wide

range of temperatures. Of course, just as any other treatment of transport, the current approach can be improved, especially in the low temperature regime, where the temperature-independent mobility has recently been found. Work in this direction is in progress.

## ■ APPENDIX: EXPLICIT EXPRESSIONS FOR THE CORRELATION FUNCTIONS

The expression of the correlation functions  $\langle V_{k'+q,k+q} V_{k,k'}(t) \rangle$  is mainly composed of three parts as

$$\langle V_{k_1,k_2} V_{q_1,q_2}(t) \rangle = X_{k_1,k_2;q_1,q_2} + Y_{k_1,k_2;q_1,q_2} + \Lambda_{k_1,k_2;q_1,q_2} \quad (\text{A1})$$

First, the expression of  $X_{k_1,k_2;q_1,q_2}$  is given by

$$\begin{aligned} X_{k_1,k_2;q_1,q_2} = & \sum_{k_3,k_4} [J_{k_3} J_{k_4} \langle T_{k_3,k_1;k_3,k_2} T_{k_4,q_1;k_4,q_2} \rangle \\ & - \frac{1}{N} \sum_{Q_2} J_{k_3} \omega_{Q_2} f_{-k_4}^{Q_2} \cdot (A_{-q_1}^{Q_2} \langle T_{k_3,k_1;k_3,k_2} T_{k_4+Q_2,q_1;k_4,q_2-Q_2} \rangle \\ & + A_{-q_1}^{Q_2*} \langle T_{k_3,k_1;k_3,k_2} T_{k_4+Q_2,q_1+Q_2;k_4,q_2} \rangle) \\ & - \frac{1}{N} \sum_{Q_1} J_{k_4} \omega_{Q_1} f_{-k_3}^{Q_1} \cdot (A_{-k_1}^{Q_1} \langle T_{k_3+Q_1,k_1;k_3,k_2-Q_1} T_{k_4,q_1;k_4,q_2} \rangle \\ & + A_{-k_1}^{Q_1*} \langle T_{k_3+Q_1,k_1+Q_1;k_3,k_2} T_{k_4,q_1;k_4,q_2} \rangle) \\ & + \frac{1}{N^2} \sum_{Q_1,Q_2} \omega_{Q_1} \omega_{Q_2} f_{-k_3}^{Q_1} f_{-k_4}^{Q_2} \\ & \times (A_{-k_1}^{Q_1} A_{-q_1}^{Q_2} \langle T_{k_3+Q_1,k_1;k_3,k_2-Q_1} T_{k_4+Q_2,q_1;k_4,q_2-Q_2} \rangle \\ & + A_{-k_1}^{Q_1} A_{-q_1}^{Q_2*} \langle T_{k_3+Q_1,k_1;k_3,k_2-Q_1} T_{k_4+Q_2,q_1+Q_2;k_4,q_2} \rangle \\ & + A_{-k_1}^{Q_1*} A_{-q_1}^{Q_2} \langle T_{k_3+Q_1,k_1+Q_1;k_3,k_2} T_{k_4+Q_2,q_1;k_4,q_2-Q_2} \rangle \\ & + A_{-k_1}^{Q_1*} A_{-q_1}^{Q_2*} \langle T_{k_3+Q_1,k_1+Q_1;k_3,k_2} T_{k_4+Q_2,q_1+Q_2;k_4,q_2} \rangle) \end{aligned} \quad (\text{A2})$$

where

$$\begin{aligned} \langle T_{k_1,k_2;k_3,k_4} T_{q_1,q_2;q_3,q_4}(t) \rangle = & \langle \theta_{k_1,k_2}^+ \theta_{k_3,k_4} \theta_{q_1,q_2}^+(t) \theta_{q_3,q_4}(t) \rangle \\ & - \langle \theta_{k_1,k_2}^+ \theta_{k_3,k_4} \rangle \langle \theta_{q_1,q_2}^+ \theta_{q_3,q_4} \rangle \end{aligned} \quad (\text{A3})$$

and the expressions for  $\langle \theta_{k_1,k_2}^+ \theta_{k_3,k_4} \theta_{q_1,q_2}^+(t) \theta_{q_3,q_4}(t) \rangle$  and  $\langle \theta_{k_1,k_2}^+ \theta_{k_3,k_4} \rangle \langle \theta_{q_1,q_2}^+ \theta_{q_3,q_4} \rangle$  have been given by eq 38 and eq 33, respectively. Here and onward,  $N$  represents the total number of sites used in the transport calculation.

Now we turn to the expression of  $Y_{k_1,k_2;q_1,q_2}$ , which is written as

$$\begin{aligned} Y_{k_1,k_2;q_1,q_2} = & \sum_{k_3,k_4} \left\{ \frac{1}{\sqrt{N}} \left[ \sum_Q J_{k_3} \omega_Q f_{-k_4}^Q \langle Z_{k_1,k_3;k_3,k_2} \psi_Q(t) \rangle \right. \right. \\ & \times \langle T_{k_3,k_1;k_3,k_2} T_{k_4+Q,q_1;k_4,q_2}(t) \rangle - \frac{1}{N} \sum_{Q_1,Q_2} \omega_{Q_1} \omega_{Q_2} f_{-k_3}^{Q_1} f_{-k_4}^{Q_2} \\ & \times (A_{-k_1}^{Q_1} \langle Z_{k_1,k_3+Q_1;k_3,k_2-Q_1} \psi_{Q_2}(t) \rangle \\ & \times \langle T_{k_3+Q_1,k_1;k_3,k_2-Q_1} T_{k_4+Q_2,q_1;k_4,q_2}(t) \rangle \\ & + A_{-k_1}^{Q_1*} \langle Z_{k_1,k_3+Q_1,k_3+Q_1;k_3,k_2} \psi_{Q_2}(t) \rangle \end{aligned}$$

$$\begin{aligned}
& \times \langle T_{k_3 + Q_1, k_1 + Q_1; k_3, k_2} T_{k_4 + Q_2, q_1; k_4, q_2}(t) \rangle \\
& + \frac{1}{\sqrt{N}} \left[ \sum_{Q_1} J_{k_4} \omega_{Q_1} f_{-k_3}^{Q_1} \cdot \langle \psi_{Q_1} Z_{q_1, k_4; k_4, q_2}(t) \rangle \right. \\
& \times \langle T_{k_3 + Q_1, k_1; k_3, k_2} T_{k_4, q_1; k_4, q_2}(t) \rangle - \frac{1}{N} \sum_{Q_1, Q_2} \omega_{Q_1} \omega_{Q_2} f_{-k_3}^{Q_1} f_{-k_4}^{Q_2} \\
& \times (A_{-q_1}^{Q_2} \langle \psi_{Q_1} Z_{q_1, k_4 + Q_2; k_4, q_2 - Q_2}(t) \rangle \\
& \times \langle T_{k_3 + Q_1, k_1; k_3, k_2} T_{k_4 + Q_2, q_1; k_4, q_2 - Q_2}(t) \rangle \\
& + A_{-q_1}^{Q_2*} \langle \psi_{Q_1} Z_{q_1 + Q_2, k_4 + Q_2; k_4, q_2}(t) \rangle \\
& \left. \times \langle T_{k_3 + Q_1, k_1; k_3, k_2} T_{k_4 + Q_2, q_1 + Q_2; k_4, q_2}(t) \rangle \right] \quad (A4)
\end{aligned}$$

where

$$\begin{aligned}
& \langle C_{k_1, k_2; k_3, k_4} \psi_q(t) \rangle \\
& = \frac{1}{\sqrt{N}} \{ A_{-k_2}^{k_1 - k_2} [n e^{-i\omega t} - (1+n)e^{i\omega t}] \delta_{-k_1 + k_2, q} \\
& - A_{-k_4}^{k_3 - k_4} [n e^{-i\omega t} - (n+1)e^{i\omega t}] \delta_{-k_3 + k_4, q} \} \quad (A5)
\end{aligned}$$

and

$$\begin{aligned}
& \langle \psi_q Z_{k_1, k_2; k_3, k_4}(t) \rangle = \frac{1}{\sqrt{N}} \{ A_{-k_2}^{k_1 - k_2} [(n+1)e^{i\omega t} \\
& - n e^{-i\omega t}] \delta_{q, -k_1 + k_2} - A_{-k_4}^{k_3 - k_4} [(n+1)e^{i\omega t} \\
& - n e^{-i\omega t}] \delta_{q, -k_3 + k_4} \} \quad (A6)
\end{aligned}$$

Here  $n$  is the Bose–Einstein distribution, with  $2n + 1 = \coth(1/2\beta\hbar\omega)$ .

Finally, we give the expression of  $\Lambda_{k_1, k_2; q_1, q_2}$ :

$$\begin{aligned}
& \Lambda_{k_1, k_2; q_1, q_2} = \sum_{k_3, k_4} \frac{1}{N} \left\{ \sum_{Q_1, Q_2} \omega_{Q_1} \omega_{Q_2} f_{-k_3}^{Q_1} f_{-k_4}^{Q_2} \right. \\
& \times \left\{ \frac{1}{N} (-A_{-k_3 - Q_1}^{k_1 - k_3 - Q_1} A_{-k_4 - Q_2}^{q_1 - k_4 - Q_2} \delta_{k_1 - k_3 - Q_1, -Q_2} \delta_{-Q_1, q_1 - k_4 - Q_2} \right. \\
& + A_{-k_3 - Q_1}^{k_1 - k_3 - Q_1} A_{-q_2}^{k_4 - q_2} \delta_{k_1 - k_3 - Q_1, -Q_2} \delta_{Q_1, q_2 - k_4} \\
& + A_{-k_2}^{k_3 - k_2} A_{-k_4 - Q_2}^{q_1 - k_4 - Q_2} \delta_{k_2 - k_3, Q_2} \delta_{-Q_1, q_1 - k_4 - Q_2} \\
& \left. - A_{-k_2}^{k_3 - k_2} A_{-q_2}^{k_4 - q_2} \delta_{k_2 - k_3, Q_2} \delta_{Q_1, q_2 - k_4} \right\} \cdot \\
& [n e^{-i\omega t} - (n+1)e^{i\omega t}]^2 + \langle \psi_{Q_1} \psi_{-Q_2}(t) \rangle \delta_{Q_1, -Q_2} \} \cdot \\
& \langle T_{k_3 + Q_1, k_1; k_3, k_2} T_{k_4 + Q_2, q_1; k_4, q_2}(t) \rangle \quad (A7)
\end{aligned}$$

## AUTHOR INFORMATION

### Corresponding Author

\*Electronic address: YZhao@ntu.edu.sg.

## ACKNOWLEDGMENT

Support from the Singapore Ministry of Education through the Academic Research Fund (Tier 2) under Project No. T207B1214 and the Singapore National Research Foundation through the Competitive Research Programme (CRP) under Project No. NRF-CRP5-2009-04 is gratefully acknowledged.

## REFERENCES

- (1) Pope, M.; Swenberg, C. E. *Electronic Processes in Organic Crystals and Polymers*, 2nd ed.; Oxford University Press: Oxford, U.K., 1999; pp 337–340.
- (2) Heeger, A. J.; et al. *Rev. Mod. Phys.* **1988**, 60, 781.
- (3) Nelson, S. F.; et al. *Appl. Phys. Lett.* **1998**, 72, 1854.
- (4) Lin, Y. Y.; et al. *IEEE Electron Device Lett.* **1997**, 18, 606.
- (5) Dimitrakopoulos, C.; et al. *Science* **1999**, 283, 822.
- (6) Garnier, F.; Horowitz, G.; Peng, X. Z.; Fichou, D. *Adv. Mater.* **1990**, 2, 592.
- (7) Holstein, T. *Ann. Phys.* **1959**, 8, 325.
- (8) Holstein, T. *Ann. Phys.* **1959**, 8, 343.
- (9) Silinsh, E.; V. Čápek, *Organic Molecular Crystals: Interaction, Localization, and Transport Phenomena*; American Institute of Physics: New York, 1994.
- (10) Glaeser, R. M.; Berry, R. S. *J. Chem. Phys.* **1966**, 44, 3797.
- (11) Silbey, R.; Munn, R. W. *J. Chem. Phys.* **1980**, 72, 2763.
- (12) Munn, R. W.; Silbey, R. *J. Chem. Phys.* **1985**, 83, 1843.
- (13) Silbey, R.; Munn, R. W. *J. Chem. Phys.* **1985**, 83, 1854.
- (14) Mahan, G. D. *Many-Particle Physics*; Kluwer Academic/Plenum Publishers: New York, 2010.
- (15) Kenkre, V. M.; et al. *Phys. Rev. Lett.* **1989**, 62, 1165.
- (16) Fratini, S.; Ciuchi, S. *Phys. Rev. Lett.* **2003**, 91, 256403.
- (17) Coropceanu, V.; et al. *Chem. Rev.* **2007**, 107, 926.
- (18) Cheng, Y. C.; Silbey, R. *J. Chem. Phys.* **2008**, 128, 114713.
- (19) Munn, R. W.; Silbey, R. *Mol. Cryst. Liq. Cryst.* **1980**, 57, 131.
- (20) Yarkony, D. R.; Silbey, R. *J. Chem. Phys.* **1976**, 65, 1042.
- (21) Yarkony, D. R.; Silbey, R. *J. Chem. Phys.* **1977**, 67, 5818.
- (22) Ortmann, F.; Bechstedt, F.; Hannewald, K. *Phys. Rev. B* **2009**, 79, 235206.
- (23) Warta, W.; Karl, N. *Phys. Rev. B* **1985**, 32, 1172.
- (24) Zhao, Y.; Brown, D. W.; Lindenberg, K. *J. Chem. Phys.* **1994**, 100, 2335.
- (25) Zhao, Y.; Li, G. Q.; Sun, J.; Wang, W. H. *J. Chem. Phys.* **2008**, 129, 124114. Liu, Q. M.; Zhao, Y.; Wang, W. H.; Kato, T. *Phys. Rev. B* **2009**, 79, 165105.
- (26) Sun, J.; Zhao, Y.; Liang, W. Z. *Phys. Rev. B* **2009**, 79, 155112.
- (27) Wang, D.; et al. *J. Chem. Phys.* **2010**, 132, 081101.
- (28) Parris, P. E.; Kenkre, V. M. *Phys. Rev. B* **2004**, 70, 064304.
- (29) Hannewald, K.; et al. *Phys. Rev. B* **2004**, 69, 075211.
- (30) Hannewald, K.; Bobbert, P. A. *Appl. Phys. Lett.* **2004**, 85, 1535.
- (31) Hannewald, K.; et al. *Phys. Rev. B* **2004**, 69, 075212.
- (32) Ortmann, F.; Bechstedt, F.; Hannewald, K. *New J. Phys.* **2010**, 12, 023011.
- (33) Ortmann, F.; Bechstedt, F.; Hannewald, K. *J. Phys.: Condens. Matter* **2010**, 22, 465802.
- (34) Ortmann, F.; Hannewald, K.; Bechstedt, F. *Appl. Phys. Lett.* **2008**, 93, 222105.
- (35) Ortmann, F.; Hannewald, K.; Bechstedt, F. *J. Phys. Chem. B* **2009**, 113, 7367.
- (36) Giuggioli, L.; Andersen, J. D.; Kenkre, V. M. *Phys. Rev. B* **2003**, 67, 045110.
- (37) Hultell, M.; Stafstrom, S. *Chem. Phys. Lett.* **2006**, 428, 446.
- (38) Troisi, A.; Orlandi, G. *Phys. Rev. Lett.* **2006**, 96, 086601.
- (39) Grover, M. K.; Silbey, R. *J. Chem. Phys.* **1970**, 52, 2099.
- (40) Zhao, Y.; Brown, D. W.; Lindenberg, K. *J. Chem. Phys.* **1997**, 106, 2728.
- (41) Zhao, Y.; Brown, D. W.; Lindenberg, K. *J. Chem. Phys.* **1997**, 107, 3159.
- (42) Fratini, S.; Ciuchi, S. *Phys. Rev. Lett.* **2009**, 103, 266601.
- (43) Alvermann, A.; et al. *Phys. Rev. B* **2010**, 81, 165113.